

Intracrine testosterone activation in human pancreatic β cells stimulates insulin secretion.

Weiwei Xu¹, Lina Schiffer², M.M. Fahd Qadir¹, Yanqing Zhang¹, James Hawley³, Paula Mota De Sa¹ Brian G Keevil³, Hongju Wu¹, Wiebke Arlt^{2,4}, Franck Mauvais-Jarvis^{1,5}

¹Department of Medicine, Section of Endocrinology and Metabolism, Tulane University Health Sciences Center, ²Institute of Metabolism and Systems Research, University of Birmingham, Birmingham, B15 2TT, UK; ³Department of Clinical Biochemistry, Wythenshawe Hospital, Manchester National Health Service Foundation Trust, Manchester, M23 9LT, UK; ³National Institute for Health Research (NIHR) Birmingham Biomedical Research Centre, University of Birmingham and University Hospitals Birmingham NHS Foundation Trust, Birmingham, B15 3GW, UK; ²Southeast Louisiana Veterans Affairs Healthcare System, New Orleans, LA 70112, USA;

Running title: Intracrine testosterone metabolism and insulin secretion

Tweet: Human pancreatic #betacells locally produce active androgens and estrogens from circulating testosterone to stimulates insulin production #diabetes @FMauvaisJarvis @TulaneMedicine

***Correspondance:** Franck Mauvais-Jarvis, MD, Ph.D. Department of Medicine, Section of Endocrinology and Metabolism, Tulane University Health Sciences Center, 1430 Tulane Avenue, New Orleans, LA 70112, U.S.A. Email: fmauvais@tulane.edu

Abstract

Testosterone (T) affects β cell function in men and women. T is a pro-hormone that undergoes intracrine conversion in target tissues to the potent androgen dihydrotestosterone (DHT) via the enzyme 5 α -reductase (5 α -R), or to the active estrogen 17 β -estradiol (E2) via the aromatase enzyme. Using male and female human pancreas sections, we show that the 5 α -R type1 isoform (SRD5A1) and aromatase are expressed in male and female β cells. We show that cultured male and female human islets exposed to T produce DHT and downstream metabolites. In these islets, exposure to the 5 α -R inhibitors finasteride and dutasteride inhibited T conversion into DHT. We did not detect T conversion into E2 from female islets. However, we detected T conversion into E2 in islets from one out of four male donors. In this donor, exposure to the aromatase inhibitor anastrozole inhibited E2 production. Notably, in cultured male and female islets, T enhanced glucose-stimulated insulin secretion (GSIS). In these islets, exposure to 5 α -R inhibitors or the aromatase inhibitor both inhibited T enhancement of GSIS. In conclusion, male and female human islets convert T into DHT and E2 via the intracrine activities of SRD5A1 and aromatase. This process is necessary for T enhancement of GSIS.

Introduction

Accumulated evidence suggests that the gonadal steroid testosterone (T) is necessary for proper glucose-stimulated insulin secretion (GSIS) in men and promotes insulin hypersecretion and β cell dysfunction in women with androgen excess (1-4). Accordingly, the active metabolite of T, dihydrotestosterone (DHT), enhances GSIS in cultured islets from male human donors (3). Male mice lacking the androgen receptor (AR) selectively in β cells (β ARKO) exhibit impaired GSIS, leading to glucose intolerance, and develop diabetes (3). In addition, exposure of cultured islets from female human donors to DHT promotes insulin hypersecretion (4). In a female mouse model of chronic androgen excess, DHT promotes hyperinsulinemia associated with secondary pancreatic β cell dysfunction via action on AR in β cells (4).

In healthy men and hyperandrogenic women, T is the main circulating gonadal androgen. T is a weak androgen and a pro-hormone that undergoes local conversion in target tissues to either DHT via action of one of the 5α -reductase (5α -R) isoforms (5), or 17β -estradiol (E2) via action of the enzyme aromatase, to activate AR or estrogen receptor(ER)s, respectively (5, 6). Notably, activation of ERs by E2 in male and female human β cells enhances insulin synthesis, GSIS, and promotes survival from multiple metabolic injuries (7-11). Therefore, circulating T could have a clinically relevant impact on β cell function in healthy men and hyperandrogenic women via conversion to DHT and/or E2 within pancreatic islets. However, the extent to which 5α -R isoforms and the aromatase are present in human islets from both sexes and able to convert T to DHT and E2 to directly affect β cell function is unknown.

Here, we have used pancreas sections and cultured islets from male and female human donors to study the expression of the three 5α -R isoforms and the aromatase, quantify

the conversion of T to DHT and E2 and assess the functional significance of intracrine conversion of T in pancreatic islets on GSIS.

Research Design and Methods

Immunohistochemistry. Human pancreas sections were obtained from the Network for Pancreas Organ Donors with Diabetes (nPOD). Sections went through deparaffinization and antigen retrieval, followed by incubation with primary antibodies. Insulin (1:100, Abcam) staining from pancreas sections was performed as described (9). For steroidogenic enzyme staining, sections were incubated in primary antibody, anti-aromatase (1:50, Novus), anti-SRD5A1 (1:50, Abcam), anti-SRD5A2 (1:50, Santa Cruz), and anti-SRD5A3 (1:50, Abcam) and then incubated in the goat anti-rabbit secondary antibody (1:300). Images were taken using a Nikon A1 confocal microscope.

Human islet steroid conversion assays. Human islets were obtained from the Integrated Islet Distribution Program (IIDP) (see **Supplementary Table 1** for donor information) and were recovered overnight in complete medium: RPMI-1640 (Gibco) supplemented with 10% charcoal-stripped FBS and Pen/Strep (100 U/ml, 100 µg/ml). Islets were treated with T (100nM; Sigma), the 5 α -R inhibitors finasteride (100nM; Sigma) and dutasteride (100nM; Sigma), the aromatase inhibitor anastrozole (100nM; Sigma), or vehicle (ethanol and DMSO). Other control conditions included culture medium without FBS, complete medium with finasteride and dutasteride or with anastrozole. Culture medium and islets were harvested for further analysis after a 24-hour incubation period. For normalization of the steroid concentrations to total protein content of the pancreatic islet incubations, islet cells were lysed in 2x lysis buffer (Cell Signalling) supplemented with 1 mM PMSF, 0.1 M DTT and protease inhibitor mix (Roche). Protein content of the lysate was quantified in the supernatant using the Pierce™ 660nm Protein Assay (ThermoFisher).

Steroid quantification by ultra-high-performance liquid-chromatography tandem mass spectrometry (UHPLC-MS/MS). Mass spectrometry-based analysis of steroids was performed with islets from 8 donors (4 male and 4 female). For each donor, islet incubations were performed in technical triplicates. For the measurement of androgens, 500 μ L of culture medium or external standard mix were combined with an internal standard mixture and extracted by liquid-liquid extraction with tert-butyl methyl ether (Acros Organics). For the measurement of E2, 200 μ L of sample or external standard were diluted with 150 μ L of deionised water and mixed with the internal standard. Samples were extracted by supported liquid extraction (Biotage®) with methyl tert-butyl ether (Fisher Scientific). Chromatographic separation and steroid quantification were performed using an ACQUITY ultra performance liquid chromatography system (Waters) coupled to a XEVO™ TQ-XS triple quadrupole mass spectrometer (Waters). Mass-to-charge transitions monitored in multiple reaction monitoring used for quantification are summarized in **Supplementary Table 2**. Peak area ratios of analyte and internal standard, 1/x weighting and linear least square regression were used to produce the standard curves for quantification. Limits of quantifications were 0.24 nM for T, 2.8 nM for androstenedione (A4), 0.24 nM for 5 α -dihydrotestosterone (DHT), 0.8 nM for 5 α -androstanedione (Adione), 0.8 nM for androsterone (An) and 10 pM for E2. The limit of detection for E2 was 5 pM. Additional details on UHPLC-MS/MS method are provided in Supplementary Methods.

Measurement of insulin secretion in static incubation. Human islets were hand-picked under a dissection microscope, and treated with finasteride (100nM; Sigma), dutasteride (100nM; Sigma), anastrozole (100nM; Sigma), or vehicle for 6 hours prior to adding steroids. Testosterone (10nM; Sigma), DHT (10nM; Steraloids), E2 (10nM M; Steraloids) or vehicle were then added at 2.8mM and then 16.7mM glucose for 40

minutes sequentially. Insulin release from islets was measured with Human Insulin ELISA kit (Millipore Sigma) as described (9). See **Supplementary Table 1** for donor information.

Statistics. Statistical analyses were performed with GraphPad Prism. When results showed a Gaussian distribution, one-way ANOVA (with Bonferroni post hoc test) was performed. Results were expressed as the mean \pm SEM, and $P < 0.05$ was considered to be significant. Significance was expressed as follows: * $P < 0.05$, ** $P < 0.01$, *** $P < 0.001$.

Data and Resource Availability

Data supporting the results reported in the article will be shared upon request. Resource reported in the article will be shared upon request.

Results

Expression of 5 α -R and aromatase enzymes in human islets

We examined the expression of the aromatase enzyme, CYP19A1, a member of the cytochrome P450 superfamily of enzymes, and 5 α -R isoforms in pancreas sections from male and female nondiabetic human donors. Three isoforms of 5 α -R exist: 5 α -R type 1 (SRD5A1), 5 α -R type 2 (SRD5A2) and 5 α -R type 3 (SRD5A3) (12). SRD5A1 showed expression in the cytoplasm of β cells in male and female islets without expression in α cells or in adjacent exocrine cells (**Fig. 1**). We did not observe reliable expression of SRD5A2 or SRD5A3 in either male or female islet cells (**Supplementary Fig.1**). The aromatase was expressed in the cytoplasm of β cells and possibly in other non- α β islet cells and with minimal exocrine location in both male and female human islets (**Fig. 1**). The expression of SRD5A1 and CYP19A1 in human β cells was confirmed using publicly available datasets of RNA-seq from whole pancreas, bulk islets and FACS purified β cells (**Supplementary Fig.1**). Interestingly, at the mRNA level, SRD5A1 expression was higher in females than in males.

Human islets can metabolize testosterone into active steroids

We treated cultured islets from male and female human donors with T and quantified the conversion of T to androgenic and estrogenic metabolites by ultra-high performance liquid-chromatography tandem mass spectrometry (UHPLC-MS/MS). **Fig. 2A** illustrates the possible T conversion pathways: T can be converted by 5 α -reduction to DHT and by 17 β -hydroxysteroid dehydrogenase (17 β HSD) activity to androstenedione (A4). A4 is further converted to its downstream metabolites, 5 α -androstenedione (Adione) and androsterone, by sequential 5 α -R and 3 α -hydroxysteroid dehydrogenase (3 α -HSD) activities. T can also be aromatized to E2.

After treatment of cultured male and female human islets with T, we detected and quantified DHT in the culture supernatant (**Fig. 2 B and C**). DHT was not detected when islets were co-treated with the potent 5 α -R inhibitors, Finasteride and Dutasteride (12) (**Fig. 2 B and C**). However, DHT was detected when islets were co-treated with the selective aromatase inhibitor, Anastrozole (6, 13) (**Fig. 2 B and C**). This demonstrates that human islets of both sexes can convert T to DHT via 5 α -R activity.

In addition, in the culture supernatants of T-treated male and female islets, we detected the presence of A4, consistent with 17 β HSD activity in these islets. Notably, male and female islets treated with T also produced Adione and androsterone (**Fig. 2 D and E**), and these metabolites were not detected when islets were treated with 5 α -R inhibitors but were still detected when islets were treated with the aromatase inhibitor (**Fig. 2 D and E**). This demonstrates that human islets of both sexes can convert A4 into Adione via 5 α -R activity. In addition, we observed the formation of androsterone, a downstream metabolite of Adione.

Despite immunohistochemical and transcriptomic evidence of aromatase expression in male and female human islets (**Fig. 1**) and β cells (**Supplementary Fig. 2.**), we did not detect E2 in the culture media of T-treated female islets. However, we detected E2 in the media of T-treated islets from two of four male donors, irrespective of absence or presence of 5 α -R inhibitors (**Fig. 3**). For one of them (Male 4, **Fig. 3**), E2 was detectable in all incubations with T and T plus 5 α -R inhibitors; In 5 of those 6 incubations E2 concentrations could be accurately quantified and ranged from 12 to 32 pmol/L. For the other male islet donor (Male 1, **Fig. 3**) we could detect E2 concentrations below the limit of quantification but clearly above the limit of detection in one of the three technical replicates incubated with testosterone and in all three replicates incubated with testosterone and 5 α -R inhibitors (**Fig. 3**). Notably, E2 was not detected in either donor when islets were co-incubated with T and aromatase inhibitor (**Fig. 3**).

Inhibition of SRD5A1 and aromatase activities prevent T amplification of GSIS

Having observed that male and female human islets express SRD5A1 and aromatase and convert T to DHT, and in males also to E2, we next examined the physiological relevance of intracrine T metabolism to male and female human islet function in an experiment assessing GSIS in static incubation. At 16.7 mM glucose, male and female human islets exposed to T showed increased GSIS to an extent similar to those exposed to DHT compared to those exposed to vehicle only (**Fig. 4A and C**). Notably, exposure of T-treated male and female islets to the 5 α -R inhibitors Finasteride and Dutasteride blocked the effect of T in amplifying GSIS (**Fig. 4A and C**). Consistent with the expression of SRD5A1 in β cells, exposure of T-treated islets to Finasteride alone (SRD5A2 and 3 inhibitor) had no effect on T enhancement of GSIS compared to vehicle. In contrast, in the presence of Dutasteride alone (SRD5A1, 2 and 3 inhibitor), the ability of T to amplify GSIS compared to vehicle was no longer significant (**Supplementary Fig. 3**). Additionally, at 16.7 mM glucose, male human islets exposed to E2 showed increased GSIS to an extent similar to those exposed to T compared to those exposed to vehicle only (**Fig. 4B**). Importantly, despite the lack of E2 detection in the T-treated islets, but consistent with the presence of aromatase in human islets, as shown above (**Fig. 1 and Supplementary Fig. 2**), the aromatase inhibitor Anastrozole blocked the ability of T to amplify GSIS (**Fig. 4B**). Similar results were obtained in islets from female human donors (**Fig. 4C and D**). Together these data demonstrate that T acutely amplifies GSIS in male and female human islets and that the insulinotropic effect of T requires 5 α -reduction to DHT and aromatization to E2.

Discussion

Original studies by Jean Wilson and others in male subjects with undervirilization led to the discovery that T requires conversion to DHT by SRD5A2 for masculinization of the male external genitalia (14, 15). Beyond masculinization, however, T also exhibits important metabolic actions including effects on insulin secretion (2, 16, 17).

We show that human islets from both sexes can convert T to DHT via the enzyme SRD5A1 expressed in β -cells. SRD5A2 is involved in sexual development and is primarily localized to classical androgen target tissues, whereas SRD5A1 is expressed in skin and other extra-genital androgen target tissues (5). Our finding that treatment with 5 α -R inhibitors abolishes T-induced increase in GSIS demonstrates that in β cells, T acts primarily as a prohormone, requiring conversion to DHT by SRD5A1 to exert its actions. Therefore, in healthy men, circulating T provides a precursor for intracrine activation to DHT in β cells to stimulate insulin production (3). Notably, 5 α -R inhibitors are used to treat benign prostatic hyperplasia (BPH), a disease affecting approximately 50% of older men. Men with BPH exposed to the 5 α -R inhibitors finasteride and dutasteride exhibit an increased risk of developing new onset type 2 diabetes compared to men receiving the α -blocker tamsulosin (18). Taken together, these data suggest that 5 α -R inhibitors, by blocking T conversion to DHT in β cells, promote β cell dysfunction, thus predisposing to new onset type 2 diabetes.

In women with androgen excess, various degrees of β cell dysfunction have been described (2, 19-21) and circulating testosterone concentrations are closely linked to risk of type 2 diabetes in women (22, 23). In female mice with androgen excess, chronic AR activation in β cells promotes insulin hypersecretion and β cell dysfunction (4). Our finding that T is converted to DHT in female human islets suggests that intracrine androgen activation also plays an important role in mediating these adverse effects of T on β cell function in women.

Despite evidence of aromatase expression in male and female β cells, E2 was not detected in the culture media of T-treated female islets, although we were able to detect it in the supernatant of one out of four T-treated male islet cultures. It is conceivable that the islets of the three other donors formed low levels of E2, but the resulting E2 concentrations were below the limit of detection of our E2 assay (10 pM). Alternatively, following an intracrine principle, E2 locally produced in the β cell could directly and efficiently interact with ERs in the same β cells followed by inactivation in the same cells (24). Most importantly, and consistent with efficient conversion of T into E2 in β cells in both sexes, T enhancement of GSIS from cultured male and female islets was blunted after co-incubation with the aromatase inhibitor anastrozole. Consistent with islet conversion of T to E2, anastrozole abolished E2 production by the male islets with detectable E2 production at baseline. Taken together, these findings show that T also requires aromatization to E2 to enhance GSIS. Surprisingly, 5 α -R and aromatase inhibitors similarly abolish the ability of T to enhance GSIS suggesting that both DHT and E2 signaling pathways are necessary to this effect. E2 and DHT activate multiple signaling pathways in β cell metabolism (3, 4, 7-11), which may act synergistically to produce the optimal effect of T on GSIS in males and female β cells (25).

In conclusion, using highly selective and specific tandem mass spectrometry assays we show for the first time that human pancreatic islets can locally activate androgens and estrogens from circulating T, and that this activity is localized to β cells. We show that these local steroid metabolic pathways drive GSIS, thereby establishing an intracrine mode of sex steroid action in β cells.

Acknowledgments

This work was supported by grants from the National Institutes of Health (DK074970 and DK107444 to F.M.J., DK107412 to H.W.), a U.S. Department of Veterans Affairs Merit Review Award (BX003725) to F.M.J., a Wellcome Trust Investigator Award (209492/Z/17/Z) to W.A., and the National Institute for Health Research (NIHR) Birmingham Biomedical Research Centre at the University Hospitals Birmingham NHS Foundation Trust and the University of Birmingham (Grant BRC-1215-20009). This research was performed with the support of the Network for Pancreatic Organ donors with Diabetes (nPOD; RRID:SCR_014641), a collaborative type 1 diabetes research project sponsored by JDRF (nPOD: 5-SRA-2018-557-Q-R) and The Leona M. & Harry B. Helmsley Charitable Trust (Grant#2018PG-T1D053). The content and views expressed are the responsibility of the authors and do not necessarily reflect the official view of nPOD, the NIHR or the Department of Health and Social Care UK. Organ Procurement Organizations (OPO) partnering with nPOD to provide research resources are listed at <http://www.jdrfnpod.org/for-partners/npod-partners/>. Human islets were provided by the Integrated Islet Distribution Program (IIDP) funded by the National Institute of Diabetes and Digestive and Kidney Diseases and with support from the Juvenile Diabetes Research Foundation International.

WX designed and performed experiments of IHC and GSIS, analyzed the data, prepared the figures and wrote the manuscript. LS performed steroid conversion experiments including androgen profiling by UHPLC-MS/MS, analyzed the data, and edited the manuscript. MMFQ and PMDS performed experiments of GSIS in human islets. YZ performed experiments of IHC from pancreas sections. JH and BGK performed estradiol measurements by UHPLC-MS/MS. HW performed experiments and analysis of IHC images from pancreas sections, prepared figure 1 and edited the manuscript. WA

designed and provided interpretation of the steroid conversion experiments and edited the manuscript. FMJ designed the study, analyzed the data, wrote and revised the manuscript. FMJ is the guarantor of this work and, as such, had full access to all the data in the study and takes responsibility for the integrity of the data and the accuracy of the data analysis. The authors have no conflicts of interest to declare.

References

1. Mauvais-Jarvis F. Androgen-deprivation therapy and pancreatic beta-cell dysfunction in men. *J Diabetes Complications*. 2016;30(3):389-90.
2. Xu W, Morford J, Mauvais-Jarvis F. Emerging role of testosterone in pancreatic β cell function and insulin secretion. *J Endocrinol*. 2019;240(3):R97.
3. Navarro G, Xu W, Jacobson DA, Wicksteed B, Allard C, Zhang G, et al. Extranuclear Actions of the Androgen Receptor Enhance Glucose-Stimulated Insulin Secretion in the Male. *Cell Metab*. 2016;23(5):837-51.
4. Navarro GN, Allard C, Morford JJ, Xu W, Liu S, Molinas AJ, et al. Androgen excess in pancreatic β -cells and neurons predisposes to type 2 diabetes in female mice. *JCI Insight*. 2018.
5. Wilson JD, Griffin JE, Russell DW. Steroid 5 α -Reductase 2 Deficiency*. *Endocrine Reviews*. 1993;14(5):577-93.
6. Santen RJ, Brodie H, Simpson ER, Siiteri PK, Brodie A. History of Aromatase: Saga of an Important Biological Mediator and Therapeutic Target. *Endocrine Reviews*. 2009;30(4):343-75.
7. Liu S, Kilic G, Meyers MS, Navarro G, Wang Y, Oberholzer J, et al. Oestrogens improve human pancreatic islet transplantation in a mouse model of insulin deficient diabetes. *Diabetologia*. 2013;56(2):370-81.
8. Liu S, Le May C, Wong WP, Ward RD, Clegg DJ, Marcelli M, et al. Importance of extranuclear estrogen receptor-alpha and membrane G protein-coupled estrogen receptor in pancreatic islet survival. *Diabetes*. 2009;58(10):2292-302.
9. Tiano JP, Delghingaro-Augusto V, Le May C, Liu S, Kaw MK, Khuder SS, et al. Estrogen receptor activation reduces lipid synthesis in pancreatic islets and prevents beta cell failure in rodent models of type 2 diabetes. *J Clin Invest*. 2011;121(8):3331-42.
10. Tiano JP, Mauvais-Jarvis F. Importance of oestrogen receptors to preserve functional beta-cell mass in diabetes. *Nat Rev Endocrinol*. 2012;8(6):342-51.
11. Xu B, Allard C, Alvarez-Mercado AI, Fuselier T, Kim JH, Coons LA, et al. Estrogens Promote Misfolded Proinsulin Degradation to Protect Insulin Production and Delay Diabetes. *Cell Rep*. 2018;24(1):181-96.
12. Azzouni F, Godoy A, Li Y, Mohler J. The 5 alpha-reductase isozyme family: a review of basic biology and their role in human diseases. *Adv Urol*. 2012;2012:530121.
13. Geisler J. Differences between the non-steroidal aromatase inhibitors anastrozole and letrozole--of clinical importance? *Br J Cancer*. 2011;104(7):1059-66.
14. Walsh PC, Madden JD, Harrod MJ, Goldstein JL, MacDonald PC, Wilson JD. Familial Incomplete Male Pseudohermaphroditism, Type 2. *New England Journal of Medicine*. 1974;291(18):944-9.
15. Imperato-McGinley J, Guerrero L, Gautier T, Peterson RE. Steroid 5 α -Reductase Deficiency in Man: An Inherited Form of Male Pseudohermaphroditism. *Science*. 1974;186(4170):1213-5.
16. Navarro G, Allard C, Xu W, Mauvais-Jarvis F. The role of androgens in metabolism, obesity, and diabetes in males and females. *Obesity (Silver Spring)*. 2015;23(4):713-9.
17. Schiffer L, Kempegowda P, Arlt W, O'Reilly MW. MECHANISMS IN ENDOCRINOLOGY: The sexually dimorphic role of androgens in human metabolic disease. *Eur J Endocrinol*. 2017;177(3):R125-R43.

18. Wei L, Lai EC-C, Kao-Yang Y-H, Walker BR, MacDonald TM, Andrew R. Incidence of type 2 diabetes mellitus in men receiving steroid 5 α -reductase inhibitors: population based cohort study. *BMJ*. 2019;365:l1204.
19. Dunaif A, Finegood DT. Beta-cell dysfunction independent of obesity and glucose intolerance in the polycystic ovary syndrome. *J Clin Endocrinol Metab*. 1996;81(3):942-7.
20. Goodarzi MO, Erickson S, Port SC, Jennrich RI, Korenman SG. beta-Cell function: a key pathological determinant in polycystic ovary syndrome. *J Clin Endocrinol Metab*. 2005;90(1):310-5.
21. O'Meara NM, Blackman JD, Ehrmann DA, Barnes RB, Jaspan JB, Rosenfield RL, et al. Defects in beta-cell function in functional ovarian hyperandrogenism. *J Clin Endocrinol Metab*. 1993;76(5):1241-7.
22. Ruth KS, Day FR, Tyrrell J, Thompson DJ, Wood AR, Mahajan A, et al. Using human genetics to understand the disease impacts of testosterone in men and women. *Nature Medicine*. 2020;26(2):252-8.
23. O'Reilly MW, Glisic M, Kumarendran B, Subramanian A, Manolopoulos KN, Tahrani AA, et al. Serum testosterone, sex hormone-binding globulin and sex-specific risk of incident type 2 diabetes in a retrospective primary care cohort. *Clinical Endocrinology*. 2019;90(1):145-54.
24. Labrie F. All sex steroids are made intracellularly in peripheral tissues by the mechanisms of intracrinology after menopause. *J Steroid Biochem Mol Biol*. 2015;145:133-8.
25. Gannon M, Kulkarni RN, Tse HM, Mauvais-Jarvis F. Sex differences underlying pancreatic islet biology and its dysfunction. *Molecular Metabolism*. 2018;15:82-91.

Figure Legends

Figure 1. Expression of 5 α -reductase type 1 (SRD5A1) and aromatase in human islets. IHC staining of SRD5A1 (red), Aromatase (Ar, red), insulin (green) and glucagon (blue) in pancreas sections from male and female non-diabetic human donors. Representative images are shown.

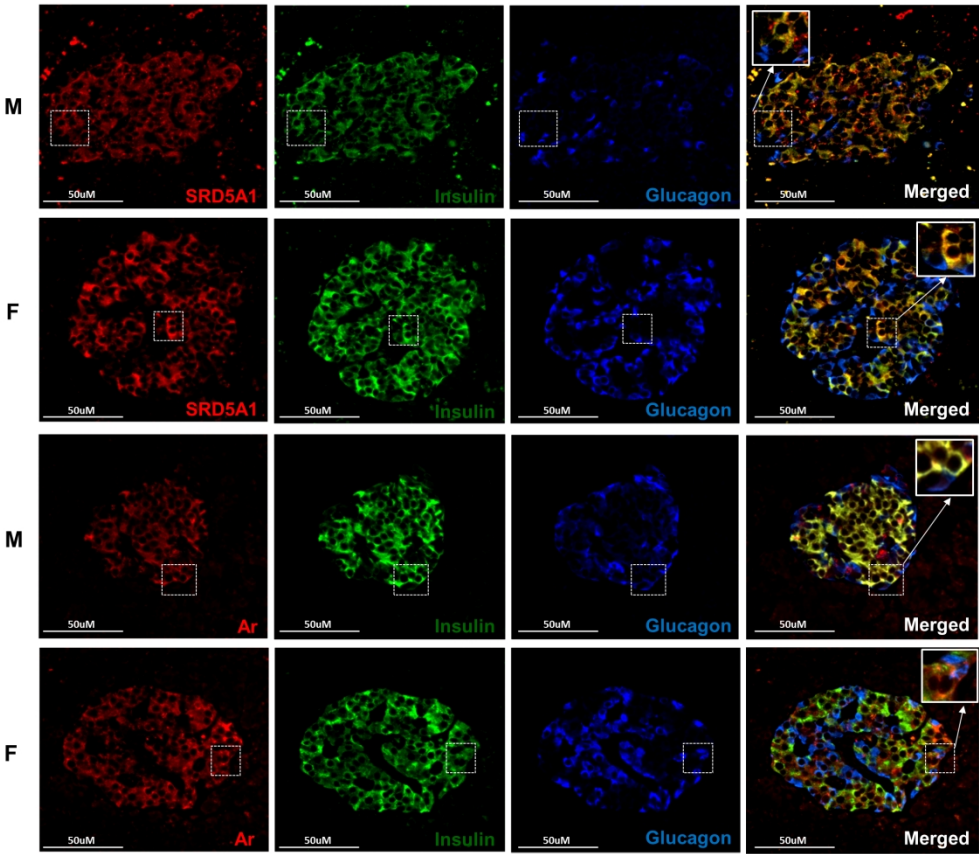
Figure 2. Human islets convert testosterone (T) to 5 α -dihydrotestosterone (DHT).

(A) Schematic presentation of the enzymatic steps involved in sex steroid metabolism. (B) Conversion of T (100nM) to DHT in male and (C) female human islets is blocked by treatment with 5 α -reductase (5 α -R) inhibitors finasteride (100nM) and Dutasteride (100nM), but unaffected by treatment with aromatase (Ar) inhibitor (anastrozole, 100nM). (D) T conversion to androstenedione (A4), followed by further conversion to 5 α -androstenedione (Adione) and androsterone (An) in male and (E) female islets, is blocked by treatment with 5 α -R inhibitors, but unaffected by Ar inhibitor treatment. Steroid concentrations were quantified by LC-MS/MS and normalized to total protein of the islet lysate. The mean \pm SEM and scatter plot of technical triplicates for each donor (4 men, 4 women) are shown. Samples with steroids concentrations <LLOQ are represented as 0. Estradiol: E2; 3 α -hydroxysteroid dehydrogenase: 3 α -HSD; 17 β -hydroxysteroid dehydrogenase: 17 β -HSD.

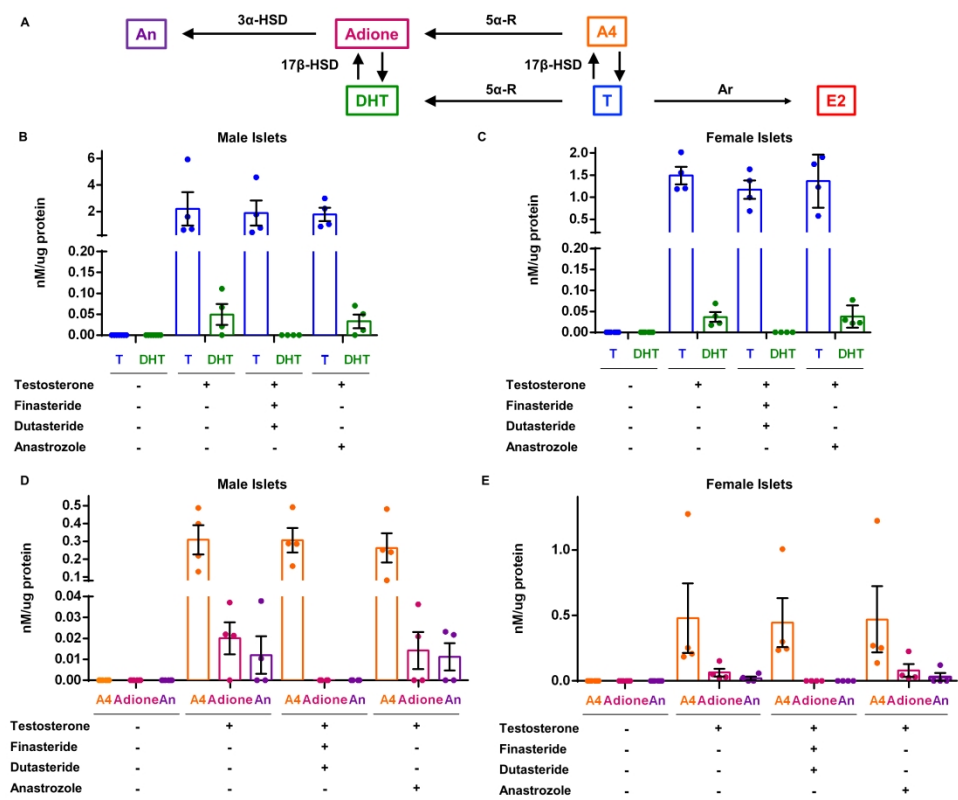
Figure 3. Male human islets convert testosterone (T) to estradiol (E2). Conversion of T (100nM) to E2 in two male donors is blocked by treatment with Ar inhibitor (anastrozole, 100nM), but retained following treatment with 5 α -R inhibitors (finasteride and dutasteride, 100nM). (A) Heat map showing quantifiable, detectable and nondetectable E2 concentrations measured by LC-MS/MS in each replicate (n=3) for

each male islet donor (n=4); **(B)** Chromatogram of the LC-MS/MS runs for all treatments and technical replicates of the two male donor islets with detectable or quantifiable E2. The arrow shows the location of the E2 peak.

Figure 4. Inhibition of SRD5A1 and aromatase prevents testosterone-induced amplification of GSIS. GSIS measured in static incubation in (A) male human islets treated with vehicle, T (10nM), 5 α -R inhibitors (finasteride and dutasteride, 100nM) and DHT (10nM); (B) male human islets treated with vehicle, T, Ar inhibitor (anastrozole, 100nM) and E2 (10nM); (C) female human islets treated with vehicle, T, 5 α -R inhibitors and DHT; (D) female human islets treated with vehicle, T, Ar inhibitor and E2. The mean \pm SEM and scatter plot of technical triplicates for each donor (4 men, 3 women) are shown. *P < 0.05, **P < 0.01, ***P < 0.001

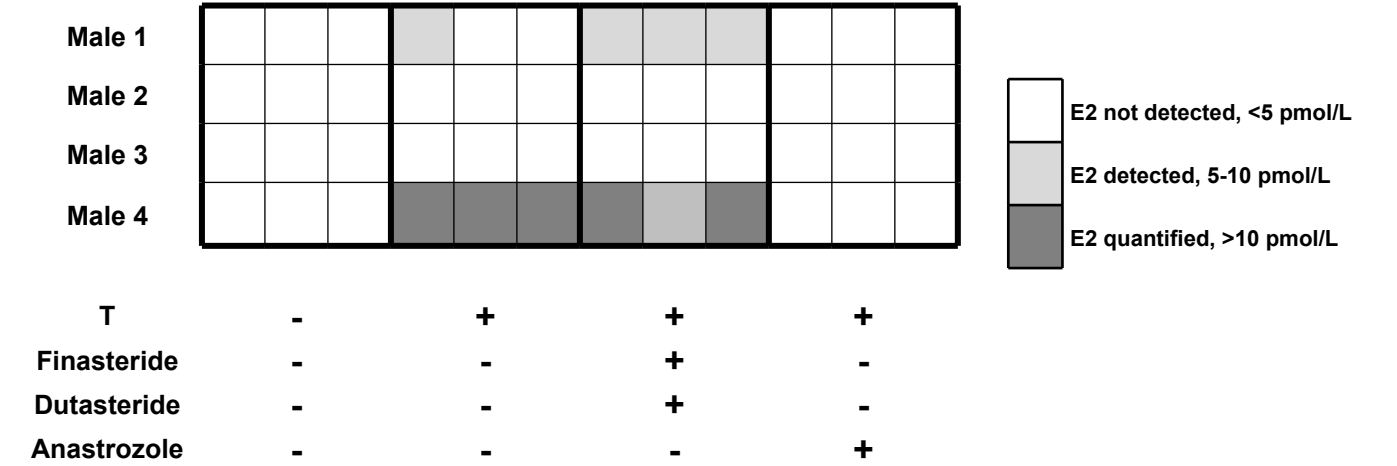


190x165mm (300 x 300 DPI)

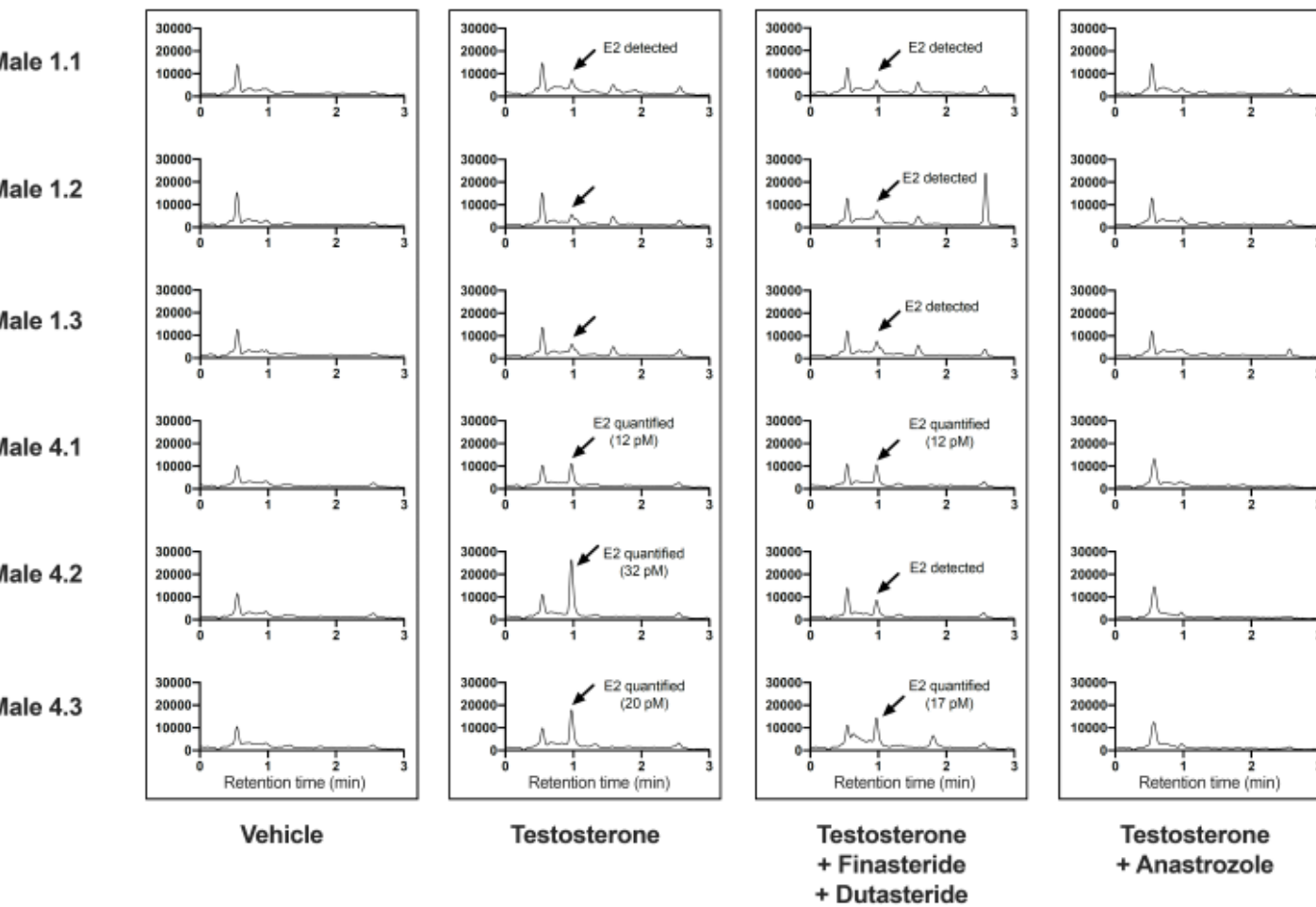


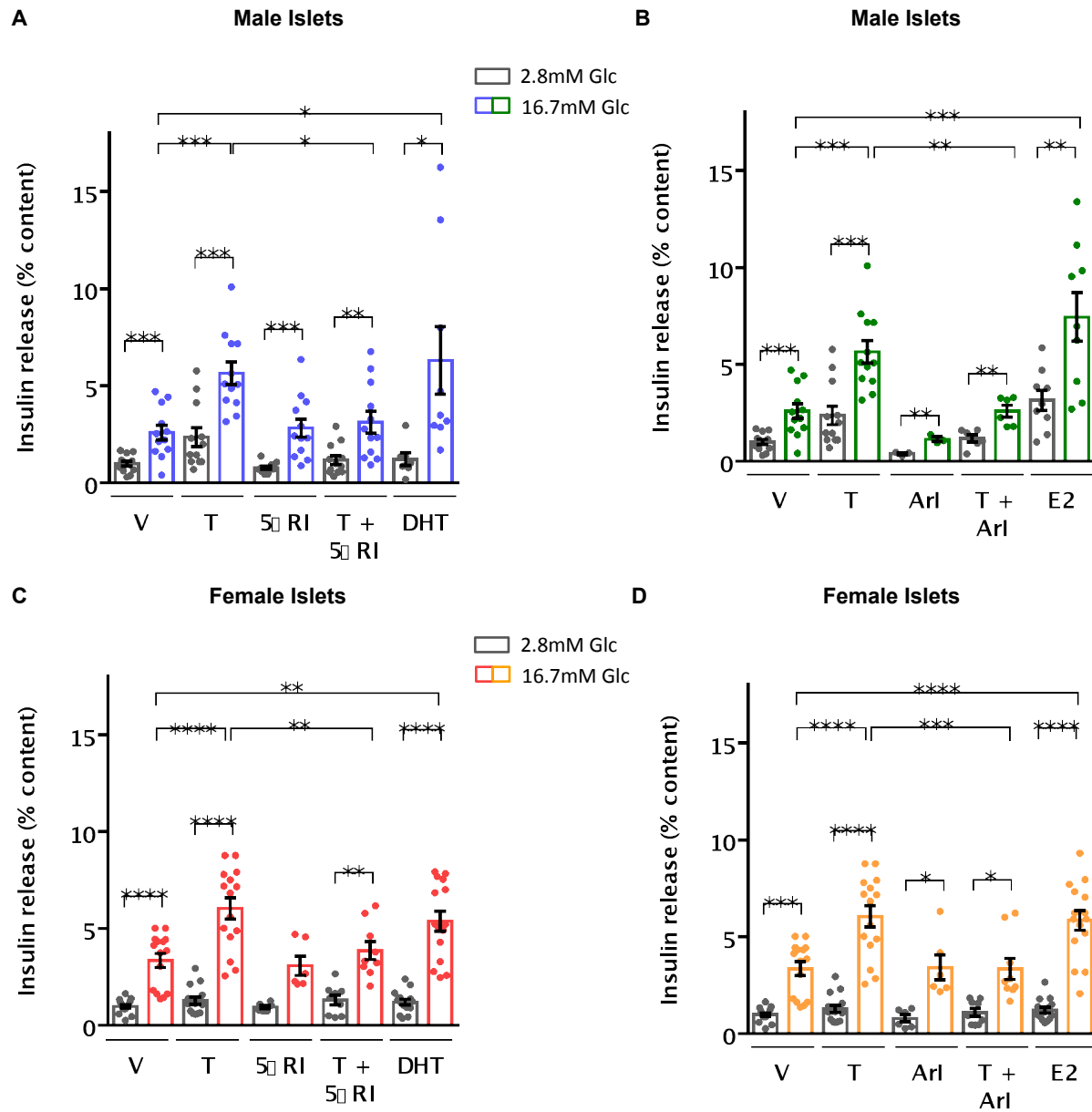
304x241mm (300 x 300 DPI)

A



B

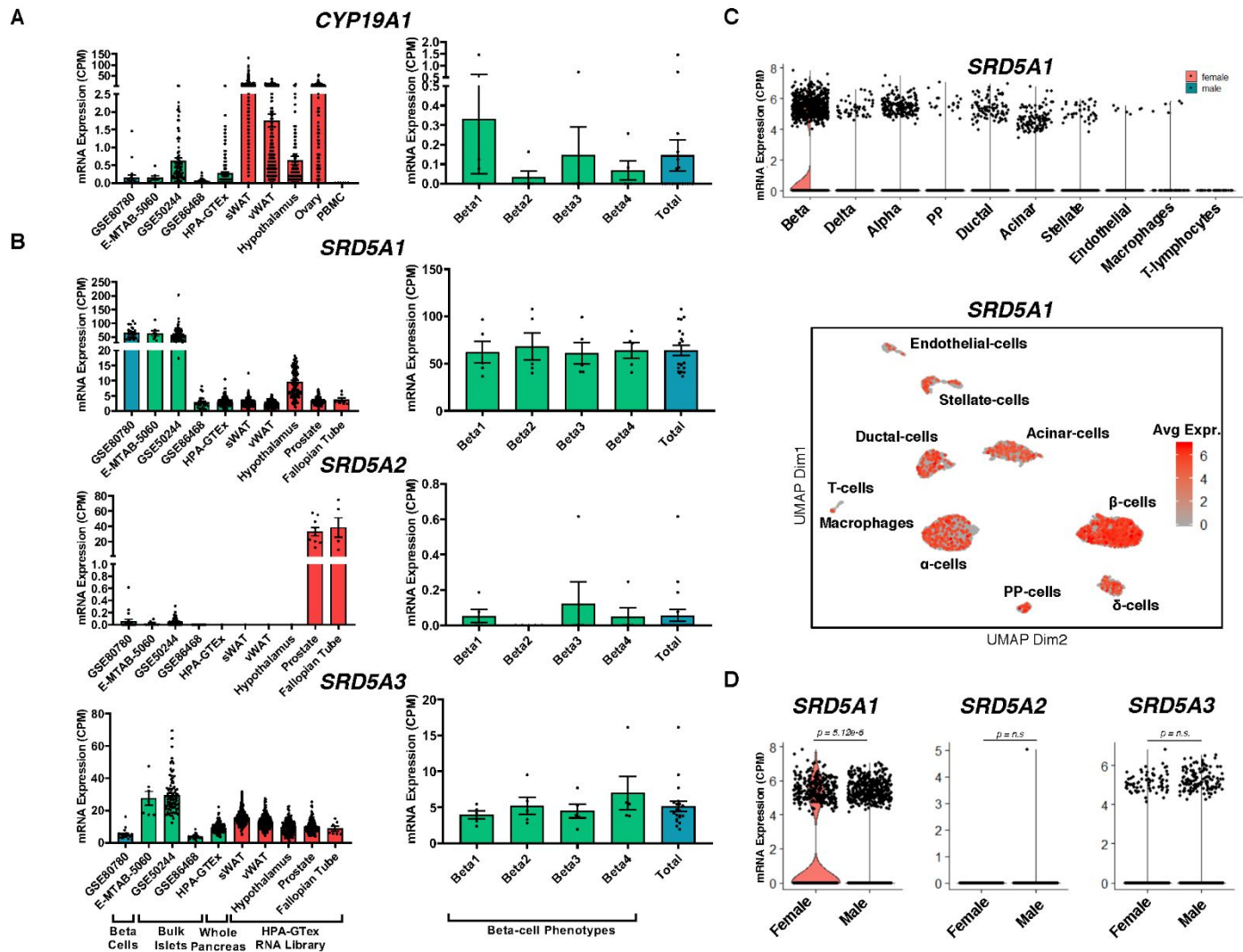




Intracrine testosterone activation in human pancreatic β cells stimulates insulin secretion.

Weiwei Xu, Lina Schiffer, M.M. Fahd Qadir, Yanqing Zhang, Paula Mota De Sa, Brian G Keevil, Hongju Wu, Wiebke Arlt, Franck Mauvais-Jarvis

Supplementary File



Supplementary Figure 1. Human pancreatic β cells expression CYP19A1 and SRD5A1-3 in RNA-seq datasets. Normalized mRNA expression of (A) CYP19A1 and (B) SRD5A1-3. Left panels represent scatter plots with mean \pm SD of mRNA expression (counts per million) from FACS sorted β cells (GSE80780), bulk islets (E-MTAB-5060, GSE50244 and GSE86468), whole pancreas (HPA-GTEx) and control tissues (sWAT: subcutaneous white adipose tissue, vWAT: visceral white adipose tissue, hypothalamus, prostate, ovary, PBMCs: peripheral blood mononuclear cells, and fallopian tubes). Right panels represent scatter plot with mean \pm SD of mRNA expression (counts per million) from FACS sorted β cells from 4 different phenotypes as described in methods, and all 4 β cell phenotypes combined (derived from GSE80780 denoted in the right panel). (C) Normalized mRNA expression of SRD5A1 in a single-cell mRNA expression atlas of pancreatic islets cells (GSE84133). Top panel represents violin plots showing the distribution of data points and probability density of their overall expression. The plots are split in two halves, the left half denoting female while the right half denoting

male expression levels. Bottom panel represents a non-linear multidimensional uniform maximal projection (UMAP) map showing expression distribution of SRD5A1 across different cell types in pancreatic islets. **(D)** Normalized mRNA expression of SRD5A1-3 in human pancreatic β cells derived from a single cell mRNA-Seq expression atlas of pancreatic islets (GSE84133). Data are represented as violin plots showing distribution of data points and the probability density of their overall expression. Information on donor numbers is provided in the methods.

Methods for Supplementary Figure 1.

Supplemental data files containing count information was downloaded from publicly available datasets (data were collectively accessed on: 4/27/2020). A description of the raw datafiles and their relevant citations is shown in the table below:

Dataset Identifier	Dataset Characteristics	Dataset link	Citation	Sample Number
GSE80780	FACS sorted human β cell subtype bulk RNAseq	https://www.ncbi.nlm.nih.gov/geo/query/acc.cgi?acc=GSE80780	¹	$n = 5$
E-MTAB-5060	Human Islet bulk RNAseq	https://www.ebi.ac.uk/arrayexpress/experiments/E-MTAB-5060/	²	$n = 5$
GSE50244	Human Islet bulk RNAseq	https://www.ncbi.nlm.nih.gov/geo/query/acc.cgi?acc=GSE50244	³⁻⁷	$n = 89$
GSE86468	Human Islet bulk RNAseq	https://www.ncbi.nlm.nih.gov/geo/query/acc.cgi?acc=GSE86468	⁸	$n = 24$
HPA-GTEx	Human tissue bulk RNAseq	https://www.proteinatlas.org/ENSG00000137869-CYP19A1/tissue https://www.proteinatlas.org/ENSG00000145545-SRD5A1/tissue	⁹⁻¹¹	$n = 7-442$

		https://www.proteinatlas.org/ENSG00000277893-SRD5A2/tissue https://www.proteinatlas.org/ENSG00000128039-SRD5A3		
GSE84133/ GSM2230757/ GSM2230758/ GSM2230759/ GSM2230760	Human islet single cell RNAseq	https://www.ncbi.nlm.nih.gov/geo/query/acc.cgi?acc=GSE84133 https://www.ncbi.nlm.nih.gov/geo/query/acc.cgi?acc=GSM2230757 https://www.ncbi.nlm.nih.gov/geo/query/acc.cgi?acc=GSM2230758 https://www.ncbi.nlm.nih.gov/geo/query/acc.cgi?acc=GSM2230759 https://www.ncbi.nlm.nih.gov/geo/query/acc.cgi?acc=GSM2230760	12	$n = 4$

In case of GSE80780, we plotted the bulk RNAseq expression profiles of 4 distinct FACS sorted β cell subtypes as identified and described in¹. Once downloaded, raw mRNA count files were converted into counts per million (CPM) using either DESeq2's¹³ normalization pipeline (bulk RNAseq data) or Seurat v3.1.4^{14,15} (single cell RNAseq data) normalization and integration pipeline for CPM using the following R function:

```
(GSE84133.integrated <- NormalizeData(GSE84133.integrated, scale.factor = 1e6, assay = 'RNA', verbose = TRUE)
```

In case of the GSE84133, a Wilcoxon t -test was run to evaluate the significance for the mRNA expression between males and females. The following code in R was used to perform this function:

```
# Extract expression matrix for all beta cells
```

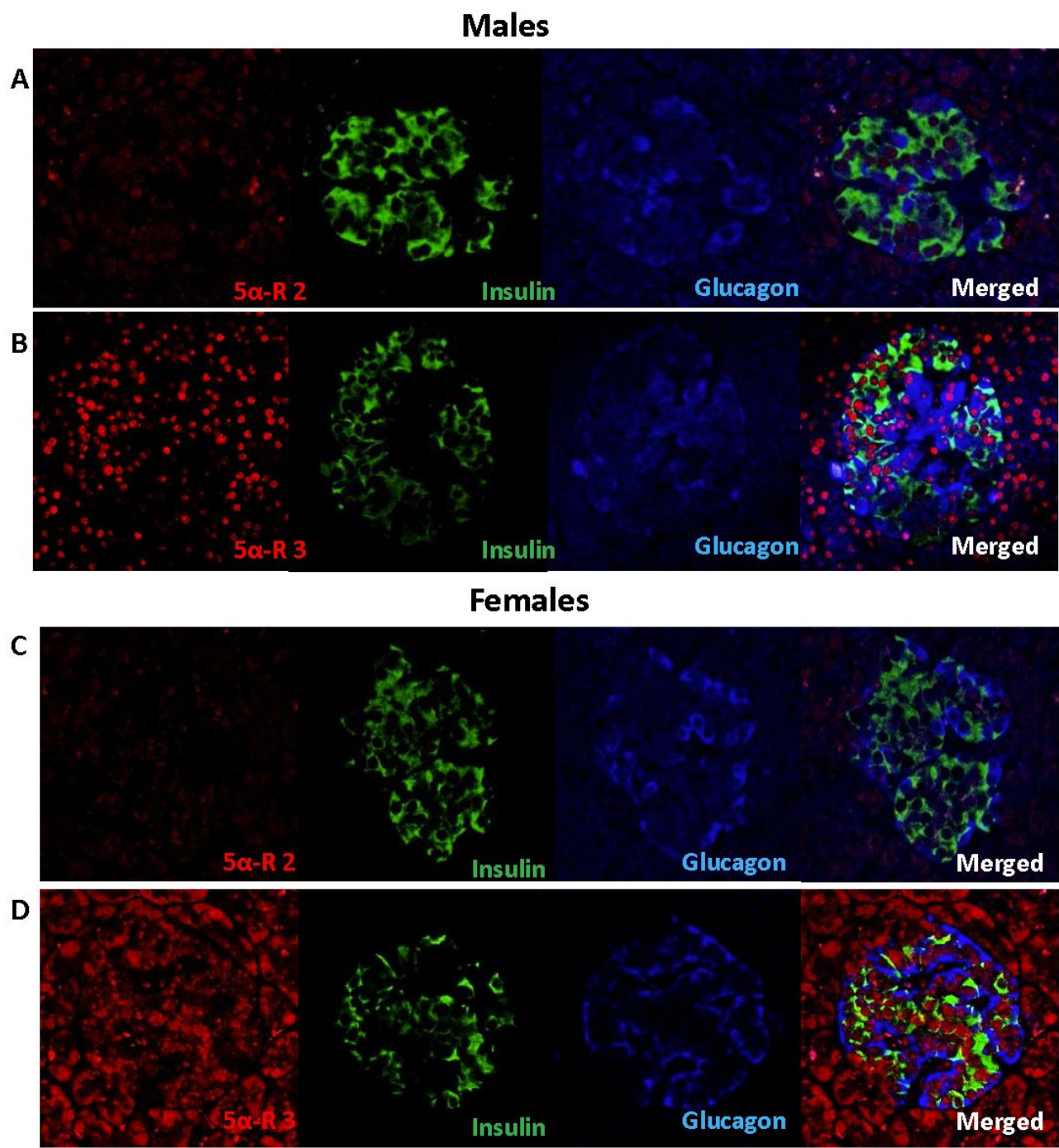
```
betacells <- subset(GSE84133.integrated, idents = c("1"))
# Set cell identity to sample identity
Idents(object = betacells) <- betacells@meta.data$sample
# Find if SRD5A1-3 genes are differentially expressed
beta.integrated.markers <- FindAllMarkers(object = betacells, slot = 'data', test.use = 'wilcox')
```

Data was then plotted using either Seurat's built in VlnPlot function or using GraphPad Prism v8.

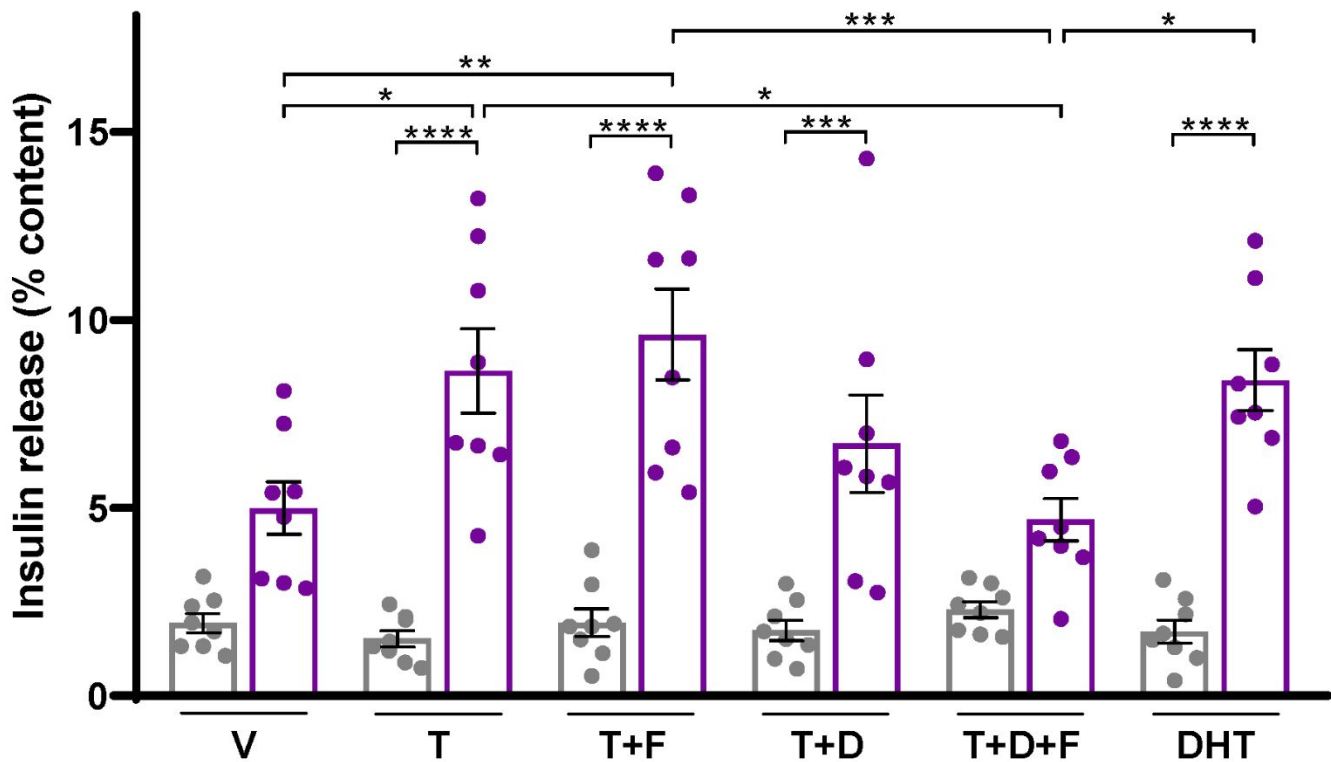
References

- 1 Dorrell, C. *et al.* Human islets contain four distinct subtypes of β cells. *Nature communications* **7**, 11756, doi:10.1038/ncomms11756 (2016).
- 2 Segerstolpe, Å. *et al.* Single-Cell Transcriptome Profiling of Human Pancreatic Islets in Health and Type 2 Diabetes. *Cell metabolism* **24**, 593-607, doi:10.1016/j.cmet.2016.08.020 (2016).
- 3 Zhou, Y. *et al.* TCF7L2 is a master regulator of insulin production and processing. *Human molecular genetics* **23**, 6419-6431, doi:10.1093/hmg/ddu359 (2014).
- 4 Fadista, J. *et al.* Global genomic and transcriptomic analysis of human pancreatic islets reveals novel genes influencing glucose metabolism. *Proceedings of the National Academy of Sciences of the United States of America* **111**, 13924-13929, doi:10.1073/pnas.1402665111 (2014).
- 5 Taneera, J. *et al.* Identification of novel genes for glucose metabolism based upon expression pattern in human islets and effect on insulin secretion and glycemia. *Human molecular genetics* **24**, 1945-1955, doi:10.1093/hmg/ddu610 (2015).
- 6 Malenczyk, K. *et al.* A TRPV1-to-secretagogue regulatory axis controls pancreatic β -cell survival by modulating protein turnover. *The EMBO journal* **36**, 2107-2125, doi:10.15252/embj.201695347 (2017).
- 7 Taneera, J. *et al.* Orphan G-protein coupled receptor 183 (GPR183) potentiates insulin secretion and prevents glucotoxicity-induced β -cell dysfunction. *Molecular and cellular endocrinology* **499**, 110592, doi:10.1016/j.mce.2019.110592 (2020).
- 8 Lawlor, N. *et al.* Single-cell transcriptomes identify human islet cell signatures and reveal cell-type-specific expression changes in type 2 diabetes. *Genome research* **27**, 208-222, doi:10.1101/gr.212720.116 (2017).
- 9 Thul, P. J. *et al.* A subcellular map of the human proteome. *Science (New York, N.Y.)* **356**, doi:10.1126/science.aal3321 (2017).
- 10 Uhlén, M. *et al.* Proteomics. Tissue-based map of the human proteome. *Science (New York, N.Y.)* **347**, 1260419, doi:10.1126/science.1260419 (2015).
- 11 Uhlen, M. *et al.* Towards a knowledge-based Human Protein Atlas. *Nature biotechnology* **28**, 1248-1250, doi:10.1038/nbt1210-1248 (2010).
- 12 Baron, M. *et al.* A Single-Cell Transcriptomic Map of the Human and Mouse Pancreas Reveals Inter- and Intra-cell Population Structure. *Cell systems* **3**, 346-360.e344, doi:10.1016/j.cels.2016.08.011 (2016).
- 13 Love, M. I., Huber, W. & Anders, S. Moderated estimation of fold change and dispersion for RNA-seq data with DESeq2. *Genome Biology* **15**, 550, doi:10.1186/s13059-014-0550-8 (2014).
- 14 Butler, A., Hoffman, P., Smibert, P., Papalexi, E. & Satija, R. Integrating single-cell transcriptomic data across different conditions, technologies, and species. *Nature biotechnology* **36**, 411-420, doi:10.1038/nbt.4096 (2018).

- 15 Stuart, T. *et al.* Comprehensive Integration of Single-Cell Data. *Cell* **177**, 1888-1902.e1821, doi:10.1016/j.cell.2019.05.031 (2019).



Supplementary Figure 2. Expression of SRD5A2 and SRD5A3 in human islets. IHC staining of SRD5A1 and SRD5A3 (red), insulin (green) and glucagon (blue) in pancreas sections from male and female non-diabetic human donors. Representative images are shown.



Supplementary Figure 3. Inhibition of SRD5A1, not SRD5A2 or 3 prevents testosterone-induced amplification of GSIS. GSIS measured in static incubation in human islets treated with vehicle, T (10nM), finasteride (F, 100nM) or dutasteride (D, 100nM), or both D +F, and DHT (10nM). The mean \pm SEM and scatter plot of technical quadruplicates from one male and one female donors are shown. *P < 0.05, **P < 0.01, ***P < 0.001.

Donor characteristics are as follows

HP-20066-01:

1. Non-diabetic
2. 60 yo
3. Female
4. Caucasian
5. 61" height
6. 139lbs weight
7. 25.8 BMI
8. Stroke COD
9. 5.1% HbA1c

HP-20071-01:

1. Non-diabetic
2. 42 yo
3. Male
4. Caucasian
5. 75" height
6. 224 lbs weight
7. 28.1 BMI
8. Head trauma COD
9. 4.9% HbA1c

Supplementary method for UHPLC-MS/MS

Both the assay for the androgen panel and the assay for E2 were validated according to industry standard (Guidance for industry. Bioanalytical method validation. US Department of Health and Human Services. Food and Drug Administration, Centre for Drug Evaluation and Research (CDER) and Centre for Veterinary Medicine (CVM), 2018).

For the androgen assay multiplexing testosterone, 5 α -dihydrotestosterone (DHT), androstenedione (A4), 5 α -androstenedione (A-dione) and 5 α -androsterone (An), the bias between nominal and measured concentrations (representing accuracy) assessed at three different concentrations was between +12 and -12% for all analytes. The coefficient of variation (%CV) for either the intra- or inter-assay imprecision, assessed for pooled biological samples and for matrix-matched samples, spiked at three different concentrations and did not exceed 8% for all analytes except androstenedione, for which it was <22%. Matrix effects were within \pm 20% across 6 samples for all analytes. Limits of quantifications were 0.24 nM for T, 2.8 nM for A4, 0.24 nM for DHT, 0.8 nM Adione and 0.8 nM for An.

For the E2 assay, the bias between nominal and measured concentrations (representing accuracy) was no greater than 8% for all 5 concentrations assessed. The coefficient of variation (%CV) did not exceed 7% for either the intra- or inter-assay imprecision at 5 different concentrations and for pooled biological samples. The assay had a mean recovery of 113% for three different concentrations assessed. The mean matrix effect across 6 samples and 3 concentrations was -12%. The limit of quantification was 10 pM and the limit of detection was 5pM. Comparison using patient serum samples against a previously published version of this assay (Owen LJ et al., Ann Clin Biochem 2014;51:360-367) showed a difference of -0.11%. The assay has been accredited against ISO 15189.

Note that we report only concentrations that are above the lower limit of quantification (LLOQ), which is the lowest concentration that can still be reliably quantified with precision (CV <20%) and accuracy (bias within \pm 20%). This is assessed during assay validation by measuring replicate samples of low concentrations.

We have applied our UHPLC-MS/MS assay in previous studies investigating steroid metabolism in other human peripheral tissues ex-vivo similar to the investigations we present here for human pancreatic islets. Our previous studies using this assay included ovarian follicles (Lebbe M et al., Endocrinology 2017, 158:1474-1485), subcutaneous adipose tissue (Markey K et al., Brain Communications 2020, 2(10), fcz050, <https://doi.org/10.1093/braincomms/fcz050>) and adrenal and gonadal tissue (Reisch N, Taylor AE et al., Proc Natl Acad Sci U S A. 2019 Oct 29;116(44):22294-22299). This information is provided in the revised Supplementary method section.

Supplemental Table 1. Islet Donor Profiles**Figure 2 & 3**

#	Receipt Date	Sex	Age (years)	Race	BMI	Cause of death
1	Nov-18	M	44	White	40	Stroke
2	Feb-19	M	25	Hispanic/Latino	27.7	Anoxia
3	May-19	M	57	Hispanic/Latino	25.8	Stroke
4	May-19	M	48	White	38.8	Stroke
5	Mar-19	F	56	N/A	39.5	Stroke
6	Mar-19	F	57	Black/African American	29.2	Stroke
7	Aug-19	F	40	White	30.4	Stroke
8	Aug-19	F	57	White	32.9	Stroke

Figure 4

#	Receipt Date	Sex	Age (years)	Race	BMI	Cause of death
1	Nov-18	M	44	White	40	Stroke
2	Nov-18	M	58	N/A	32.4	Head trauma
3	Feb-19	M	25	Hispanic/Latino	27.7	Anoxia
4	Apr-19	M	51	Hispanic/Latino	26.7	Anoxia
5	Nov-10	F	48	White	28	Stroke
6	Jan-11	F	55	Hispanic/Latino	31	Stroke
7	May-19	F	53	White	40	Stroke
8	Jan-20	F	50	White	39.2	Stroke

Supplemental Table 2. Mass-to-charge (m/z) Transitions Used for the Quantification of Andr

Steroid	m/z transitions Quantifier Qualifier
Analytes	
Testosterone	289.1 > 96.9 289.1 > 109.0
Dihydrotestosterone (DHT)	291.3 > 255.1 291.1 > 159.0
Androstenedione	287.1 > 96.9 287.1 > 108.9
5α-dione	289.2 > 271.1 289.2 > 253.1
Androsterone	291.1 > 255.1 291.1 > 273.1
Estradiol	271.4 > 145.0 271.4 > 183.0
Internal standards	
Testosterone-D3	292.1 > 96.9
DHT-D3	294.1 > 258.1
Oestradiol- ¹³ C ₃	274.4 > 148.0

rogens and Estrogen

Checklist for Reporting Human Islet Preparations Us

Adapted from Hart NJ, Powers AC (2018) Progress, challenges, and :
Report Downloaded on 3/2/2020 7:45:58 AM
Data provided by IIDP and Prodo Labs

Manuscript DOI: [insert manuscript submission number]

Title

Author list

Corresponding author

Email address

Unique identifier

Donor Age (years)

Donor Sex (M/F)

Donor BMI (kg/m²)

Donor HbA1c

Origin/source of islets

Islet isolation center^a

Donor history of diabetes? Yes/No

If Yes, complete the next two lines if this information is available

Diabetes duration (years)

Glucose-lowering therapy at time of death^b

Cause of death

Warm ischemia time (h)

Cold ischemia time (h)

Estimated purity (%)

By islet isolation center at time of shipment with Dithizone (DTZ) staining per [IIDP SOP](#)

Estimated viability (%)

By islet isolation center at time of broadcast with Fluorescence Diacetate/Propidium Iodide (FDA/PI) staining per [IIDP SOP](#)

Total culture time(h)^c

Calculate[start date/time of experiment]-[date/ time islet culture began (below)]

Date/Time Islet Culture Began at islet isolation center (Pacific Standard Time, 24-hour format)

Glucose-stimulated insulin secretion or other functional measurement^d

Stimulation Index (SI) by static incubation at islet isolation center pre-shipment per [IIDP SOP](#)

Glucose-stimulated insulin secretion or other functional measurement

Area Under the Curve (AUC) by perfusion at HIPP post shipment sample per [HIPP SOP](#)

*Shipments of more than one batch type were received from this is

^aFor example, IIDP, ECIT, Alberta IsletCore

^bPlease specify the therapy/therapies

^cTime of islet culture at the isolation centre, during shipment and at

^dPlease specify the test and the results

ised in Research

suggestions for using human islets to understand islet biology and human diabetes. Diabetologia <https://>



Intracrine testosterone activation in human pancreatic β cells stimulates insulin secretio

Weiwei Xu, Lina Schiffer, M.M. Fahd Qadir, Yanqing Zhang, Paula Mota De Sa, Brian G Ki
Franck Mauvais-Jarvis
fmauvais@tulane.edu



SAMN08776504	SAMN08786256	
	48	53
F	F	
32.3	33.2	
Not Reported	Not Reported	
IIDP	IIDP	
University of Pennsylvania	The Scharp-Lacy Research Institute	
No	No	
Not Applicable	Not Applicable	
Not Applicable	Not Applicable	



Cerebrovascular/stroke	Cerebrovascular/stroke	
Not Reported	Not Reported	
13.3	7.7	

85	85	
----	----	--

81	95	
----	----	--

Not Reported	Not Reported	
--------------	--------------	--

Not Reported	Not Reported	
--------------	--------------	--

SI (G2.8mM-G28mM)= 1.6	SI (G2.8mM-G28mM)= Not Reported	
------------------------	---------------------------------	--

AUC (G5.6mM-G16.7mM)= Not Available	AUC (G5.6mM-G16.7mM)= Not Available	
-------------------------------------	-------------------------------------	--

slet isolation

t the receiving laboratory

[//doi.org/10.1007/s00125-018-4772-2](https://doi.org/10.1007/s00125-018-4772-2).

on
eevil, Hongju Wu, Wiebke Arlt, Franck Mauvais-Jarvis

SAMN10357324	SAMN10374868	
	44	58
M	M	
40.0	32.4	
5.7	5.0	
IIDP	IIDP	
Southern California Islet Cell Resource Center	University of Wisconsin	
No	No	
Not Applicable	Not Applicable	
Not Applicable	Not Applicable	
Cerebrovascular/stroke	Head trauma	
Not Reported	Not Reported	
7.5	6.2	
75	86	
96	97	
Not Reported	Not Reported	
2018-10-31 09:00	2018-11-05 01:00	
SI (G2.8mM-G28mM)= 1.7	SI (G2.8mM-G28mM)= 3.0	

AUC (G5.6mM-G16.7mM)= 49.0 (ng/100 IEQs AUC (G5.6mM-G16.7mM)= 41.1 (ng/100 IEQs

--

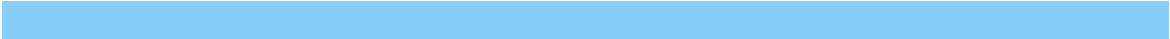
SAMN10869303	SAMN11244711	
	25	56
M	F	
27.7	39.5	
5.2	5.8	
IIDP	IIDP	
The Scharp-Lacy Research Institute	University of Wisconsin	
No	No	
Not Applicable	Not Applicable	
Not Applicable	Not Applicable	
Anoxia	Cerebrovascular/stroke	
0.5	Not Reported	
8.4	9.5	
90	94	
95	98	
Not Reported	Not Reported	
2019-01-30 19:33	2019-03-23 18:30	
SI (G2.8mM-G28mM)= 8.9	SI (G2.8mM-G28mM)= 5.3	
AUC (G5.6mM-G16.7mM)= Not Available	AUC (G5.6mM-G16.7mM)= Not Available	



MANDATORY INFORMATION		
SAMN11250012	SAMN11522709	
	57	51
F	M	
29.2	26.7	
5.2	5.7	
IIDP	IIDP	
University of Miami	Southern California Islet Cell Resource Center	
No	No	
Not Applicable	Not Applicable	
Not Applicable	Not Applicable	
RECOMMENDED INFORMATION		
Cerebrovascular/stroke	Anoxia	
0.1	0.7	
9.3	6.4	
90	85	
94	96	
Not Reported	Not Reported	
2019-03-22 22:00	2019-04-28 01:00	
SI (G2.8mM-G28mM)= 1.9	SI (G2.8mM-G28mM)= 1.9	
AUC (G5.6mM-G16.7mM)= 6.6 (ng/100 IEQs)	AUC (G5.6mM-G16.7mM)= 34.4 (ng/100 IEQs)	



SAMN11578698	SAMN11633049	
	57	48
M	M	
25.8	38.8	
5.7	5.4	
IIDP	IIDP	
The Scharp-Lacy Research Institute	University of Wisconsin	
No	No	
Not Applicable	Not Applicable	
Not Applicable	Not Applicable	



Cerebrovascular/stroke	Cerebrovascular/stroke	
Not Reported	Not Reported	
6.8	12.5	
95	90	
95	98	
Not Reported	Not Reported	
2019-05-02 17:00	2019-05-12 17:45	
SI (G2.8mM-G28mM)= 4.4	SI (G2.8mM-G28mM)= 3.2	
AUC (G5.6mM-G16.7mM)= 49.9 (ng/100 IEQs)	AUC (G5.6mM-G16.7mM)= 33.8 (ng/100 IEQs)	

--

SAMN11864195	SAMN12496804	
	53	40
F	F	
40.0	30.4	
5.5	5.0	
IIDP	IIDP	
University of Wisconsin	University of Miami	
No	No	
Not Applicable	Not Applicable	
Not Applicable	Not Applicable	
Cerebrovascular/stroke	Cerebrovascular/stroke	
Not Reported	Not Reported	
6.7	8.5	
92	90	
98	92	
Not Reported	Not Reported	
2019-05-26 10:45	2019-08-02 15:00	
SI (G2.8mM-G28mM)= 2.4	SI (G2.8mM-G28mM)= 1.0	
AUC (G5.6mM-G16.7mM)= 11.5 (ng/100 IEQs)	AUC (G5.6mM-G16.7mM)= Not Available	

--

--

SAMN12633894	SAMN13938639	
	57	50
F	F	
32.9	39.2	
5.7	5.0	
IIDP	IIDP	
Southern California Islet Cell Resource Center	Southern California Islet Cell Resource Center	
No	No	
Not Applicable	Not Applicable	
Not Applicable	Not Applicable	

--

Cerebrovascular/stroke	Cerebrovascular/stroke	
0.2	Not Reported	
5.9	11.6	

85	80	
----	----	--

96	95	
----	----	--

Not Reported	Not Reported	
--------------	--------------	--

2019-08-24 23:45	2020-01-28 01:30	
------------------	------------------	--

SI (G2.8mM-G28mM)= 1.8	SI (G2.8mM-G28mM)= Not Reported	
------------------------	---------------------------------	--

AUC (G5.6mM-G16.7mM)= 21.8 (ng/100 IEQ	AUC (G5.6mM-G16.7mM)= Not reported	
--	------------------------------------	--

HP-20043-01	64
F	
17.2	5.3
Prodo Labs	
Prodo Labs	
No	
Not Applicable	
Not Applicable	
Cerebrovascular/stroke	
	95
	95
48hrs	
	2/19/2020 2:30
SI (G2.8mM-G28mM)= Not Reported	
AUC (G5.6mM-G16.7mM)= Not reported	